Living with a Star Targeted Research and Technology

Flare Dynamics in the Lower Solar Atmosphere

Annual Team Progress Report

February 2014 to January 2015

Joel Allred (NASA GSFC)

Phil Judge (High Altitude Observatory, Lucia Kleint was PI until Sept. 2014)

Alexander Kosovichev (New Jersey Institute of Technology)

Chang Liu (New Jersey Institute of Technology)

Vahe Petrosian (Stanford University)

Haimin Wang (New Jersey Institute of Technology, Team Leader)

This is the second year of the LWS Focused Science Team (FST). Our collaborative efforts have continued to focus on the following three objectives: (1) understanding the transport of energy and momentum into the interior from the solar atmosphere during flares, (2) understanding high-energy phenomena in the impulsive phase of flares, especially the transport of high-energy particles from the corona in relation to the thick-target model, and (3) studying the changes of vector magnetic fields in the photosphere associated with flares. In this report, we summarize the progress in the aspects of organization of the team effort, highlights of scientific achievements, discussion of team events, and the tasks for the year 3.

1. Organization of Team Effort

In the past year, we organized two team meetings. The first meeting was held in Boston, on 2014 June 2, in conjunction with AAS/SPD meeting. Each team reported their research status and discussed the collaboration progress and future plan. The 2011 February 15 event was selected to be studied as the team event, as agreed by the team previously. In addition 2014 March 29 flare is added as the new team event. This flare had comprehensive coverage observations. Dr. Leamon from the NASA HQ attended the meeting.

The second meeting was held at NJIT on 2014 December 8 and 9. This is a more extended meeting. Besides presenting the progress of each team, a number of junior researchers and graduate students gave science talks on the work related to the contribution to the team effort. One of the team members, Carsten Denker, presented the status of GREGOR telescope and its capability of flare research. Dr. Dale Gary of NJIT, reported the status of EOVSA, that will be providing critical data for diagnosis of flare electrons.

2. Progress in Collaborative Projects

Allred and Petrosian groups have continued the collaboration in implementing the warm target Coulomb collision in the model. Allred made the implementation for the particle transport code by including an effective coefficient in the Fokker-Planck equation. The Petrosian group has implemented in the acceleration module the warm target Coulomb collision that adds to both the diffusion and energy loss coefficients. Allred provided improved RADYN radiative transfer hydrodynamic code to Fatima Rubio da Costa, who has been currently working on combining RADYN with the Stanford Flare code, and apply to some flares.

Petrosian team has carried out in collaborative study with Kleint on comparison of the RADYN intensity and shape of the Halpha and Ca II 8542A lines with those observed by the Dunn Solar Telescope (DST) IBIS spectro-polarimeter.

Wang and Allred teams continues a model-observation comparison in the low atmosphere flare emissions. Besides the white-light emission, the collaboration is particularly towards the understanding of black-light flares discovered with He D3 and 10830 lines. The 10830 line is already in Allred's code, while D3 will be added in the modeling. Yan Xu from Wang's team spent a week in GSFC Allred earlier in the year, now the codes have been running at NJIT cluster on campus. Recent BBSO/NST 10830 observations demonstrated black-light flares clearly.

Petrosian team continues the collaboration with Kosovichev on the hydrodynamic thick-target models and their comparison with observational results from the HMI data. They will continue the exploration of the acceleration mechanism of electrons and start on expanding the acceleration-transport code to include acceleration of protons. This will give a more accurate heating rate and can be important for analysis of flares with strong gamma-ray emission indicating a substantial contribution from protons. They will then couple this combined electron-proton acceleration code with RADYN and further investigate the feedback of the HD response on the acceleration of these particles. It will be very useful in providing an accurate assessment of momentum deposition in the photosphere and its possible role in production of seismic waves.

Kleint spent a week at NJIT to work with Chang Liu and Wang's teams. The work was mainly on the joint BBSO/NST and NSO/IBIS flare data analysis. In addition, Kleint has expertise in IRIS data analysis. This is providing very rich information on flare particle acceleration and radiative transfer.

3. Highlights of Scientific Achievements

3.1. Understanding the transport of energy and momentum into the interior from the solar atmosphere during flares

Kosovichev team's effort is focused on detection and quantitative characterization of the helioseismic response. This includes improvement of the detection methods based on finding the optimal frequency filter for the time-distance diagram method and on the holographic method of integration and reverse mapping of the point-source signal. They use both the time-distance and holography techniques. The holography method is used for an automatic detection of the signals and provides integrated characteristics, such the total egression power and its frequency dependence, but the precision for determining the localization and timing of the source are limited. The time-distance approach is more difficult to automate, but it gives detailed physical picture of the wave propagation, wave-front anisotropy, variations in the wave speed due to the interaction with sunspots and active regions, and detailed localization and initiation time and source dynamics.

The initial results include an investigation of the relationship between the holography and time-distance methods of sunquake studies. It has been shown that due to the anisotropy of the sunquake wave fronts the holography technique, which is based on the assumption that the wave propagation follows the theoretical quite-Sun model, and is isotropic, does not give correct locations of the seismic sources. To test these techniques and also to determine the location of the impact sources with height, Kosovicev et al. have performed numerical simulations using a 3D code of helioseismic wave propagation in the spherical geometry. These simulations will also allow to investigate distant effects of sunquakes.

Kosovichev team has also put significant effort in creation of the sunquake catalog analyzing all M- and X-class flares. The initial investigation included all flares of the X-ray class greater than M4.0. However, they discovered that even weaker flares of the M1-class can produce sunquakes.

A particular interesting sunquake was produced by M6.3 flare on 09/03/2012 (Kosovichev, 2014). The sunquake source was located near a neutral line outside the main delta-type configuration (Figure 1, left), but produce a very strong sunquake (Figure 1b).

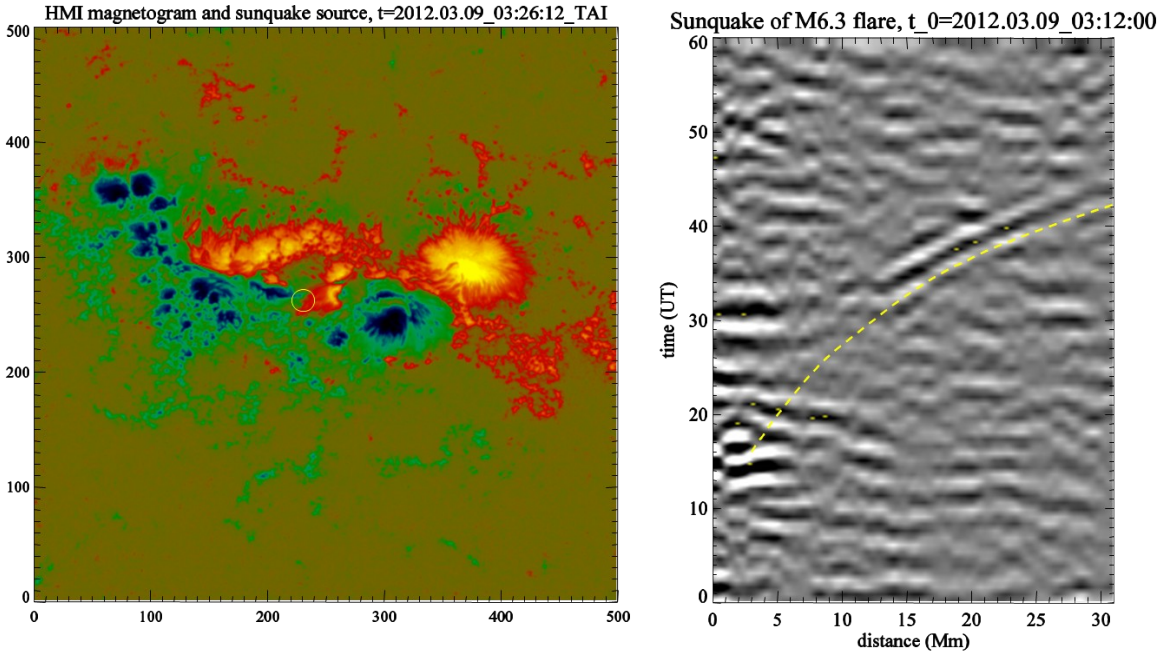

Figure 1: Location of the sunquake source (yellow circle) on the HMI magnetogram and the sunquake time-distance diagram. The sunquake source was in a weak-field region.

Also, the observations of the sunquake event in the M6.3 class flare show that the photospheric impact was at the very beginning of the flare energy release in the pre-heating phase confirming the previous finding for the X2.2 flare of Feb. 15, 2011. The photospheric Doppler velocity impulse coincides with a small peak of the soft X-ray emission. There was no significant variation of magnetic field at the impact location, and the magnetic field was very weak. This rules out the Lorentz force effects (‘McClymont jerk’), for these events.

Wang et al. (2014) reported two rarely observed three-ribbon flares (M1.9 and C9.2) on 2012 July 6 in NOAA AR 11515, using Hα observations of 0."1 resolution from the New Solar Telescope and Ca II H images from Hinode. The flaring site is characterized by an intriguing "fish-bone-like" morphology evidenced by both Hα images and a nonlinear force-free field (NLFFF) extrapolation, where two semi-parallel rows of low-lying, sheared loops connect an elongated, parasitic negative field with the sandwiching positive fields. The NLFFF model also shows that the two rows of loops are asymmetric in height and have opposite twists, and are enveloped by large-scale field lines including open fields. The two flares occurred in succession within half an hour and are located at the two ends of the flaring region. The three ribbons of each flare run parallel to the magnetic polarity inversion line, with the outer two lying in the positive field and the central one in the negative field. Both flares show surge-like flows in Hα apparently toward the remote region, while the C9.2 flare is also accompanied by EUV jets possibly along the open field lines. Interestingly, the 12-25 keV hard X-ray sources of the C9.2

flare first line up with the central ribbon then shift to concentrate on the top of the higher branch of loops. Weak sunquake was detected in one of the footpoints. These results are discussed in favor of reconnection along the coronal null line, producing the three flare ribbons and the associated ejections. The results are summarized in Figure 2.

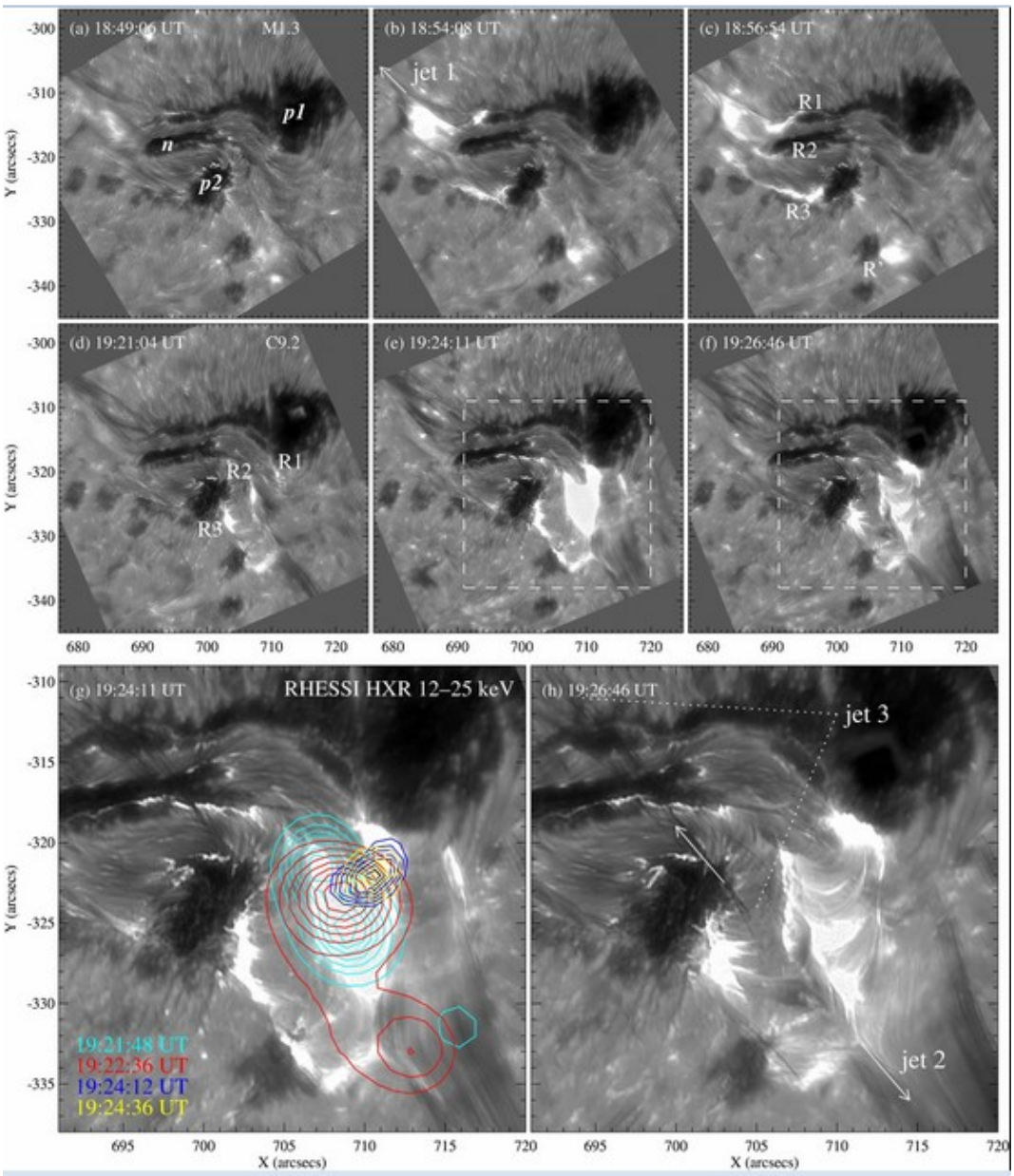

Figure 2 Time sequence of NST Hα − 0.75 Å images showing the evolution of the M1.3 (a)–(c) and C9.2 (d)–(f) flares on July 6, 2012. The dash-boxed region in panels (e) and (f) is magnified in panels (g) and (h), respectively. Contours (30%, 40%, 50%, 60%, 70%, 80%, and 90% of each maximum flux) in panel (g) represent RHESSI 12–25 keV PIXON images at the event onset and HXR peak.

Xu et al (2014) finished the paper of studying a pair of homologous flares on September 6 and 7, 2011 in AR 11283. Both of them were white-light (WL) flares as captured by the Helioseismic and Magnetic Imager (HMI) onboard Solar Dynamics Observatory (SDO), in visible continuum at 6173 A which is believed to originate from the deep solar atmosphere. They investigated the WL emission of these X-class flares with SDO's seeing-free imaging spectroscopy. The durations of impulsive peaks in the WL are less than four minutes. They compare the WL with hard X-ray (HXR) observations for the September 6 flare and find a good correlation between WL and HXR both spatially and temporally. In absence of RHESSI data during the second flare on September 7, the derivative of GOES soft X-ray (SXR) is used and also found to be well correlated with the WL. They measure the contrast enhancements, characteristic size and HXR fluxes of the twin flares. The results are similar of both flares indicating analogous triggering and heating processes. However, the September 7 flare was in accordance with conspicuous sunquake signals while there was no seismic wave detected during the preceding flare on September 06. Note that the September 7 flare has relatively weaker WL emission, indicating a softer electron beam, than that of the September 6 flare. Therefore, this comparison suggests that the particle bombard may not play an important role in creating sunquake, at least for the events studied in this paper.

Helioseismic data from the HMI instrument have revealed a sunquake associated with the X1 flare on 2014, March 29 in active region NOAA 12017. Judge et al. (2014) tried to find if acoustic-like impulses or actions of the Lorentz force caused the sunquake. They analyzed spectropolarimetric data obtained with the Facility Infrared Spectrometer (FIRS) at the DST. Stokes profiles of lines of Si I 1082.7 nm and He I 1083.0 nm are analyzed. At the flare footpoint, the Si I 1082.7 nm core intensity increases by a factor of several, the IR continuum increases by 4 ± 1%. Remarkably, the Si I core resembles the classical Ca II K line's self-reversed profile. With nLTE radiative models of H,C, Si and Fe these properties set the penetration depth of flare heating to 100 ±100 km, i.e. photospheric layers. Estimates of the non-magnetic energy flux are at least a factor of two less than the sunquake energy flux. Milne-Eddington inversions of the Si I line show that the local magnetic energy changes are also too small to drive the acoustic pulse. The work raises several questions: Have we "missed" the signature of downward energy propagation? Is it intermittent in time and/or non-local? Does the 1-2 s photospheric radiative damping time discount compressive modes?

3.2 Understanding high-energy phenomena in the impulsive phase of flares

Petrosian team's main focus of the second year has been comparison of the results from the combined code with observations. The RADYN radiative code treats the H, He, Mg and Ca atoms in non-local thermodynamic equilibrium conditions, allowing them to study their transitions in detail and to compare estimated energy fluxes with spectral observations taken with different instruments at different wavelengths. This code however, requires the input of some energy by accelerated particles. This is usually done by assuming a flux of particles with a power-law spectrum. The combined Stanford-RADYN code provide this input more accurately. In addition, they use RHESSI HXR observations to constrain the spectrum of accelerated electrons and use the accurate transport code to determine the spatial distribution of the energy deposition. The first paper on this project, carried out in collaboration with Kleint, has been on comparison of the RADYN-predicted intensity and shape of the Halpha and Ca II 8542 A lines

with those observed by the DST IBIS spectro-polarimeter. This is the most self-consistent treatment of this problem attempted so far and interesting results have been obtained. While the Ca II 8542 observations are fit adequately, the Halpha observations seem to require the presence of some micro-turbulence (Rubio da Costa et al. 2014b). Figure 3 shows representative results.

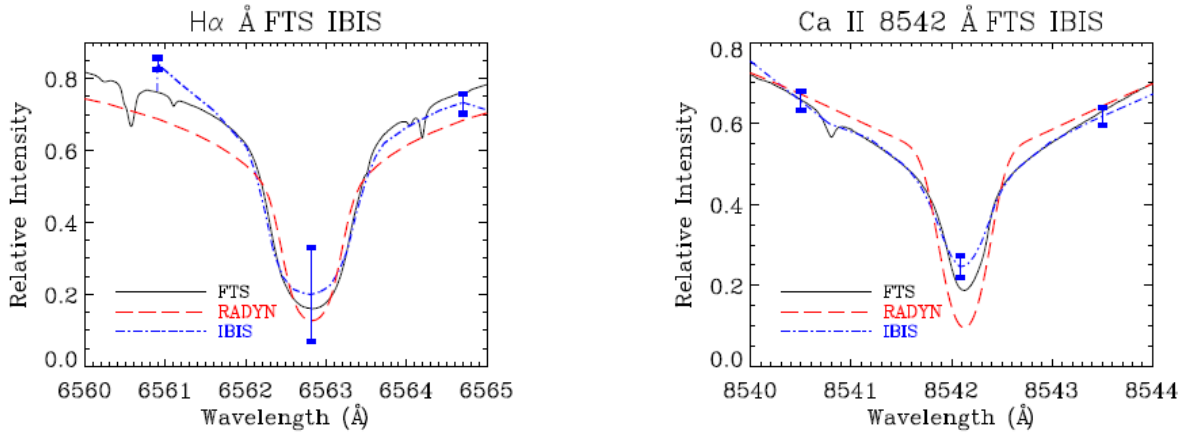

Figure 3. Comparison of the calibrated Halpha (left) and Ca II 8542 Å (right) synthetic (red solid line) and IBIS ((blue solid line) line profiles for the quiet Sun. The black solid line is the FTS atlas emission. The intensity scale is in relative units with respect to the FTS atlas continuum value. The error bars associated to the IBIS line profile represents the difference between both profiles during the flare at that particular wavelength position.

Allred team has been on concentrate on their modeling to compare with our first team event, the 2011, February 15 X2.1 flare. This event had comprehensive coverage in the observations, especially the hard X-ray of RHESSI. Hinode SOT observations provides the morphology, evolution of flare foot points. The continuum contrasts are well measured in Red (6684A), Green (5550A) and Blue (4504A) bands. Intensity and power were calculated. Using the 1D RADYN code, the radiation in a number of lines as well as continuum bands are simulated. Figure 4 shows the example comparison of WL intensity as a function of time for several different input parameters using the code. Further analyses are targeted to answer the following questions: 1. How does non- uniform ionization affect the break in the hard X-ray power law spectrum? 2. Is the ionization structure of the flaring atmosphere inferred from spectral fitting consistent with that obtained from the radiative hydrodynamic modeling? 3. Can low energy ions explain the high temperature and density inferred from the 511 keV emission line observations? 4 .What is the role of ion beams in producing white light? 5. What are the roles of ion and electron beams in producing sunquakes? 6. How does simulating a multi- looped flare arcade affect our model results? Do multi-loop flare simulations more consistently match observations?

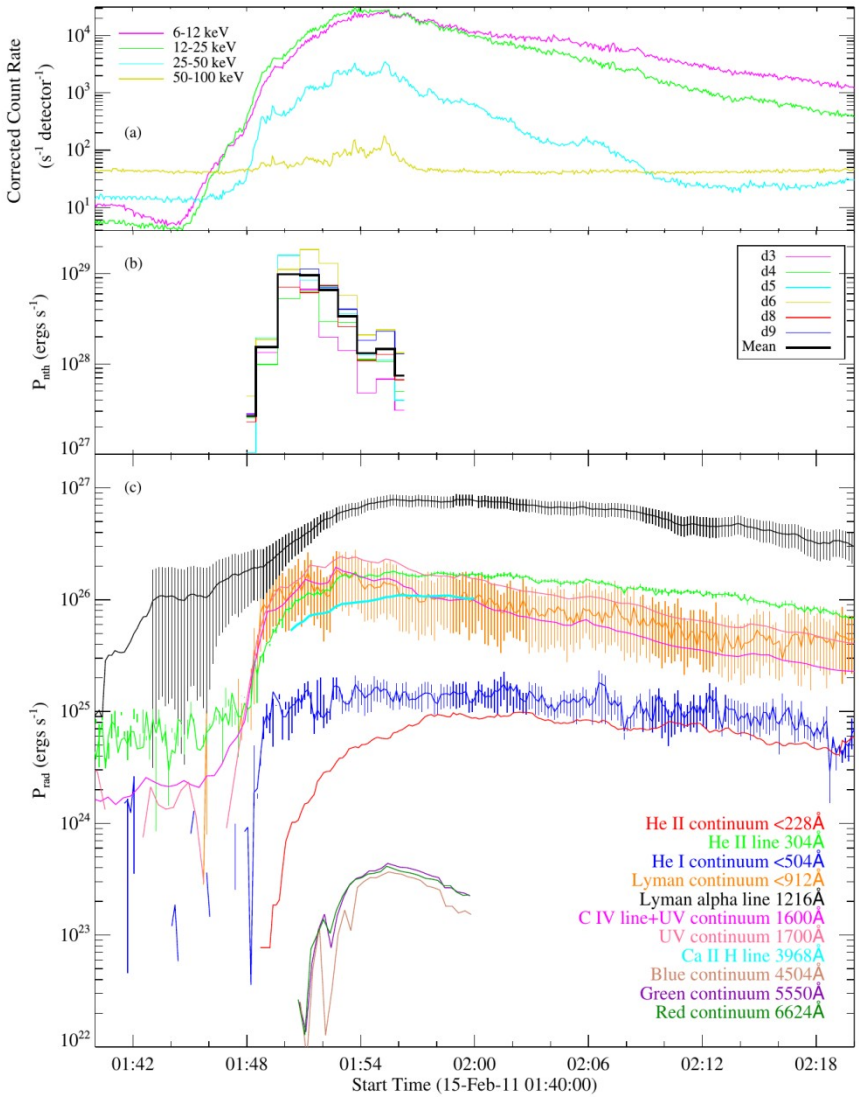

Figure 4: WL intensity as a function of time for several different input parameters using . 1D radiative hydrodynamic code.

Kleint et al. (2014) combined data from the IBIS instrument at the Dunn Solar Telescope with the spacecraft data from IRIS, Hinode, RHESSI, STEREO, and SDO in order to investigate many solar layers from the photosphere to the corona. They found a filament eruption to be the cause for this flare, and the filament's acceleration was very fast compared to previous observations. The filament's Doppler velocities were derived from the chromospheric IBIS data and increased from 2-5 km/s to 6-10 km/s about 15 minutes before the flare occurred. After the filament activation, it lifted off with at least 600 km/s, as seen in IRIS data. They also investigated small-scale structures in the IBIS data, such as a low-lying twisted flux rope, which untangled and vanished during the flare. Figure 5 shows results of observations.

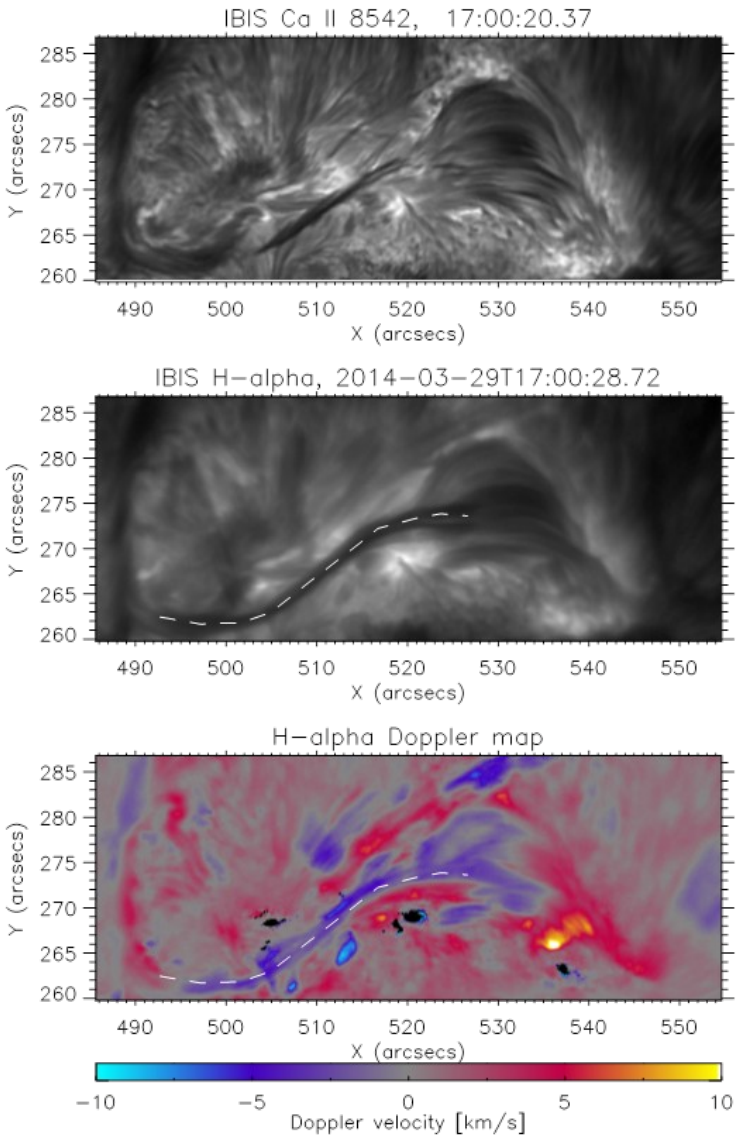

Figure 5: Top: Calcium intensity image where only the central part of the filament is visible. Middle: Hα image taken at the same time showing the whole filament with its main part marked by a dashed line. Bottom: Doppler map of Hα showing mostly blueshifts along the filament and redshifts at its western footpoint. The velocity scale was clipped at ±10 km/s.

For the first time, the Hydrogen Balmer continuum was detected from space by analyzing IRIS data from the 2014-03-29 X1 flare (Heinzel & Kleint, 2014) . Such observations will help to investigate the long-standing problem from where the continuum emission originates during flares, as accelerated electrons are not believed to reach low enough layers in the atmosphere, but their locations closely match those of continuum emission.

3.3 Studying the changes of vector magnetic fields in the photosphere associated with flares

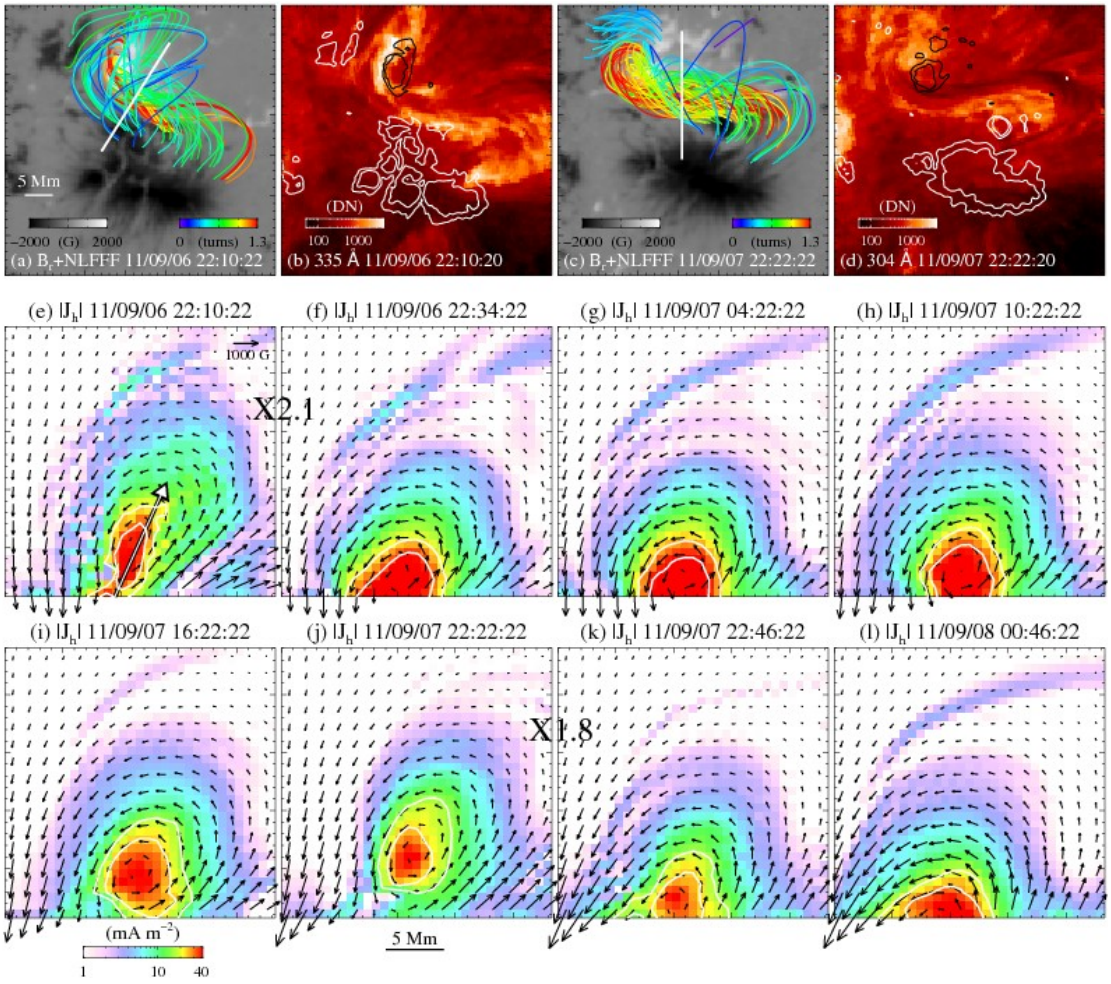

Figure 6: Preflare HMI vertical field images superimposed with selected NLFFF lines (a and c), in comparison with co-temporal AIA 304 A images (b and d) overplotted with vertical field contours at levels of ±1000 and ±1500 G. The thick white slit in (a) and (c) indicates the bottom of a rotating vertical slice of 23 × 23 Mm2, over which the distributions of Jh are plotted in (e)-(l) in logarithmic scale at selected instances. The white contours are at levels of 40% and 60% of the maximum current. The left bottom corner of the vertical slice corresponds to the southern end of the slit. The thick arrow in (e) indicates the FR orientation in the cross section. The black arrows in (e)-(l) are the transverse field vectors in the vertical slices.

Liu et al. (2014) carried out a comprehensive investigation comparing the 3D magnetic field restructuring, flare energy release, and the helioseismic response of two homologous flares, the 2011 September 6 X2.1 (FL1) and September 7 X1.8 (FL2) flares in NOAA AR 11283. In their analysis, (1) a twisted flux rope (FR) collapses onto the surface at a speed of 1.5 km/s after a partial eruption in FL1. The FR then gradually grows to reach a higher altitude and collapses again at 3 km/s after a fuller eruption in FL2. Also, FL2 shows a larger decrease of the flux-weighted centroid separation of opposite magnetic polarities and a greater change of the horizontal field on the surface. These imply a more violent coronal implosion with corresponding

more intense surface signatures in FL2. (2) The FR is inclined northward and together with the ambient fields, it undergoes a southward turning after both events. This agrees with the asymmetric decay of the penumbra observed in the peripheral regions. (3) The amounts of free magnetic energy and nonthermal electron energy released during FL1 are comparable to those of FL2 within the uncertainties of the measurements. (4) No sunquake was detected in FL1; in contrast, FL2 produced two seismic emission sources S1 and S2 both lying in the penumbral regions. Interestingly, S1 and S2 are connected by magnetic loops, and the stronger source S2 has a weaker vertical magnetic field. They discussed these results in relation to the implosion process in the low corona and the sunquake generation. The Figure 6 shows the model results and observations of the characteristic coronal field structure right before FL1 and FL2, and the aforementioned evolution of the FR during a ~1 day period.

By using the differential affine velocity estimator method and the Fourier local correlation tracking method separately, S. Wang et al. (2014) calculated velocity and vorticity of photospheric flows in the flaring NOAA AR 11158, and investigated their temporal evolution around the X2.2 flare on 2011 February 15. They found that the shear flow around the flaring magnetic polarity inversion line exhibits a sudden decrease, and both of the two main sunspots undergo a sudden change in rotational motion during the impulsive phase of the flare. These results are discussed in the context of the Lorentz-force change. This mechanism can explain the connections between the rapid and irreversible photospheric vector magnetic field change and the observed short-term motions associated with the flare. In particular, the torque provided by the horizontal Lorentz force change agrees with what is required for the measured angular acceleration.

4. Focus of Research in 2015

Our data analysis and modeling efforts will concentrate on 3 team events, all X-class flares. (1) 2011 February 15, (2) 2014 March 29 and (3) 2014 October 24. All the events have comprehensive coverage in the RHESSI HXR, make the modeling comparison feasible. Event (1) has been studied extensively. Some results on event (2) are presented in the previous sections. For event (3), the data review and some initial ideas were discussed in December 2014 team meeting. Hinode, NSO, IRIS all had good observational coverage.

Observation and Data Analysis:

- Investigate the statistical relationship between the sunquake sources detected by the time-distance and holography techniques. Investigate magnetic field and continuum emission variations in sunquake events, and also the relationship between these variations and high-energy flare emissions.

-Investigate magnetic field and continuum emission variations in sunquake events, and also the relationship between these variations and high-energy flare emissions.

- Continue spectro-polarimetric analysis of flares obtained with BBSO/NST and NSO/IBIS.
-IRIS, microwave, and hard X-ray data will be jointly analyzed.

- Study the evolution of vector magnetic fields and velocity fields associated with flares. NLFFF extrapolation tools will be utilized to understand the 3D field restructuring. The 2014 October 24 and March 29 events will be emphasized.

Modeling:

-Continue exploration of the acceleration mechanism of electrons and start on expanding the acceleration-transport code to include acceleration of protons.

-Perform initial realistic 3D simulations of the atmospheric and helioseismic responses to solar flares.

-Comparison of model results with UV lines from IRIS

-Include He D3 lines in the modeling towards a viable explanation of black-light flares.

Meetings:

Two team meetings will be planned for 2015.

5. **Publications:**

"Comparison of Emission Properties of Two Homologous Flares in AR 11283", Yan Xu, Ju Jing, Shuo Wang, and Haimin Wang, 2014, Ap.J., 787, 7

"Three-dimensional Magnetic Restructuring in Two Homologous Solar Flares in the Seismically Active NOAA AR 11283", Liu, Chang; Deng, Na; Lee, Jeongwoo; Wiegelmann, Thomas; Jiang, Chaowei; Dennis, Brian R.; Su, Yang; Donea, Alina; Wang, Haimin, 2014, Ap.J., 795, 128

"Sudden Photospheric Motion and Sunspot Rotation Associated with the X2.2 Flare on 2011 February 15", Wang, Shuo; Liu, Chang; Deng, Na; Wang, Haimin, 2014, Ap.J., Letters, 782, L31

"Study of Two Successive Three-ribbon Solar Flares on 2012 July 6", Wang, Haimin; Liu, Chang; Deng, Na; Zeng, Zhicheng; Xu, Yan; Jing, Ju; Cao, Wenda, 2014, Ap.J. Letters, 781, L23

"Fermi Detection of Gamma-ray Emission from a Behind-the-Limb M1.5 Flare on 2013 October 2011", Pesce-Rollins, M.; Omodei; N., Petrosian, V.; Liu, W.; Rubio da Costa, F. & Chen, Q.-R., 2014, ApJ Letters, to be submitted

"Combining RADYN and FLARE: modeling the solar atmosphere during solar flares", Rubio da Costa, F.; Petrosian, V; Liu, W., & Carlsson, M., 2014a, ApJ in prep.

“Solar Flare Chromospheric Line Emission: Comparison Between IBIS Observations and Radiative Transfer Hydrodynamic Simulations”, Rubio da Costa, F.; Kleint, L.; Sainz-Dalda, A.; Petrosian, V & Liu,W., 2014b, ApJ, submitted

“Evidence of nonthermal particles in coronal loops heated impulsively by nanoflares”, Testa, P.; De Pontieu, B.; Allred, J.; Carlsson, M.; Reale, F.; Daw, A.; Hansteen, V.; Martinez-Sykora, J.; Liu, W. et al. 2014, Science, Vol. 346, Issue 6207, id. 1255724

“Imaging and spectroscopic observations of magnetic reconnection and chromospheric evaporation in a solar flare”, Tian, H.; Li, G.; Reeves, K. K., Raymond, J. C.; Guo, F.; Liu, W.; Chen, B.; Murphy, N. A. 2014, ApJ Letters, in press

"On the Origin of a Sunquake during the 2014 March 29 X1 Flare"
Judge, Philip G.; Kleint, Lucia; Donea, Alina; Sainz Dalda, Alberto; Fletcher, Lyndsay
ApJ, 796, 85, 2014

"Hydrogen Balmer Continuum in Solar Flares Detected by the Interface Region Imaging Spectrograph (IRIS)" Petr Heinzel, Lucia Kleint, ApJL, 794L, 23H, 2014

"The fast filament eruption leading to the X-flare on March 29, 2014"
Lucia Kleint, Marina Battaglia, Kevin Reardon, Alberto Sainz Dalda, Peter R. Young and Sam Krucker, submitted to ApJ

“Sunquakes and Starquakes, in Precision Asteroseismology”, Kosovichev, A.G. 2013, Proc. IAU Symposium 301, Cambridge Univ. Pres.

“Sunquakes: Helioseismic Response to Solar Flares, in Extraterrestrial Seismology”, Kosovichev, A.G. 2014, Cambridge Univ. Press (in press)